Sirt1 decreased adipose inflammation by interacting with Akt2 and inhibiting mTOR/S6K1 pathway in mice[S]

Zhenjiang Liu,[1] Lu Gan,[1] Guannv Liu, Yizhe Chen, Tianjiao Wu, Fei Feng, and Chao Sun[2]

College of Animal Science and Technology, Northwest A&F University, Yangling, Shaanxi 712100, China

Abstract **Sirtuin type 1 (Sirt1) and protein kinase B (Akt2) are associated with development of obesity and inflammation, but the molecular mechanisms of Sirt1 and Akt2 interaction on adipose inflammation remain unclear. To explore these mechanisms, a mouse model was used. Mice were fed with a high-fat diet (HFD) for 8 weeks, with interventions of resveratrol (RES) or nicotinamide (NAM) during the last 15 days. The HFD reduced Sirt1 mRNA in adipose tissue and elevated interleukin-6 (IL-6) expression. RES reduced the adipose tissue weight, increased the Sirt1 mRNA level, and reduced both mRNA and protein levels of IL-6, MCP-1, inducible nitric oxide synthase, and TNF-α by inhibiting phosphorylation of Akt2 in adipose tissue. Additionally, macrophage type I marker genes were reduced while macrophage type II marker genes were elevated by RES addition. Moreover, activation of Akt2 signal by using insulin significantly blunted the inhibitory effect of RES on adipose inflammation. Immunoprecipitation assay demonstrated that RES enhances the protein-protein interaction between Sirt1 and Akt2, but NAM inhibits this interaction.[jlr] Furthermore, Sirt1 significantly reduced the levels of raptor and inactivated mammalian target of rapamycin (mTOR)C1 signal by interacting with Akt2, and confirmed that RES attenuated adipose inflammation by inhibiting the mTOR/S6K1 pathway via rapamycin.—**Liu, Z., L. Gan, G. Liu, Y. Chen, T. Wu, F. Feng, and C. Sun. **Sirt1 decreased adipose inflammation by interacting with Akt2 and inhibiting mTOR/S6K1 pathway in mice. *J. Lipid Res.* 2016.** 57: **1373–1381.**

Supplementary key words sirtuin type 1 • protein kinase B • mammalian target of rapamycin C1 • mammalian target of rapamycin/S6 kinase 1

Sirtuin type 1 (Sirt1) is a member of the silencing information regulator 2 (Sir2) family called sirtuins, and is well-known for its deacetylation in regulation of gene silencing, energy homeostasis, and apoptosis (1–3). The overloaded calorie intake leads to dysfunction of adipocytes and causes obesity (4). Obesity is closely associated with chronic inflammation and characterized by abnormal cytokine production, increased acute-phase reactants, and an activated network of inflammatory signal pathways (5). Studies have shown that Sirt1 is involved in regulation of inflammation response and inhibits inflammatory pathways in macrophages and dendritic cells (6, 7). In 3T3-L1 adipocytes, Sirt1 can attenuate TNF-α-induced insulin resistance and inflammation (3, 8). Resveratrol (RES) is a natural polyphenolic compound known for its beneficial effects on energy homeostasis (9, 10). Studies have shown that RES attenuates inflammation of adipocytes and vascular endothelial cells by activating Sirt1 and inducing autophagy (11–13). However, the regulatory mechanism of RES on Sirt1 and adipose inflammation remains unclear.

The Akt/mammalian target of rapamycin (mTOR) pathway plays an important role in the regulation of cellular gluconeogenesis and metabolism (14, 15). mTOR is highly conserved serine/threonine kinase that is expressed in cancer cells, adipocytes, and hepatocytes, and can be directly phosphorylated by activated Akt (16–18). During development of obesity, adipose pro-inflammatory responses are closely associated with the development of insulin resistance in adipose tissue (19, 20). A recent study showed that phosphorylation of Akt in macrophages could activate mTOR signal and then led to inflammation and insulin resistance in high-fat diet (HFD)-induced obesity (21). Moreover, Pang et al. (22) reported that Sirt1 directly bound protein kinase B (Akt2) and then inhibited adipogenesis in porcine adipocytes. Busch et al. (23) also suggested that Akt was one of the main upstream stimulatory kinases that modulated by Sirt1. However, whether the interaction between Sirt1 and Akt2 can regulate adipose inflammation has not been studied.

We suggested that RES would attenuate HFD-induced obesity and adipose inflammation by activating Sirt1. We found that RES promoted the interaction of Sirt1 and Akt2, and then inhibited adipose inflammation by activating the mTOR/S6K1 pathway. These findings identify a novel function of Sirt1 in the regulation of adipose inflammation

This work was supported by Major National Scientific Research Projects of China Grant 2015CB943102 and National Natural Science Foundation of China Grant 31572365.

Manuscript received 8 September 2015 and in revised form 14 June 2016.

Published, JLR Papers in Press, June 16, 2016
DOI 10.1194/jlr.M063537

Abbreviations: Akt2, protein kinase B; HFD, high-fat diet; IL-6, interleukin-6; iNOS, inducible nitric oxide synthase; mTOR, mammalian target of rapamycin; NAM, nicotinamide; RES, resveratrol; Sirt1, sirtuin type 1.

[1] Z. Liu and L. Gan contributed equally to this study.
[2] To whom correspondence should be addressed.
e-mail: sunchao2775@163.com.

[S] The online version of this article (available at http://www.jlr.org) contains a supplement.

and may offer a new potential means to prevent and treat obesity and metabolic syndrome.

MATERIALS AND METHODS

Animal studies

Six-week-old Kunming male mice were purchased from the Laboratory Animal Center of Fourth Military Medical University (Xi'an, China) and used in two experiments. The use of the animals and the animal handling protocols were approved by the Animal Ethics Committee of Northwest A&F University (Xi'an, China). All mice were provided with ad libitum water and fed a standard laboratory chow diet (F4031; Bio-Serv, Flemington, NJ) initially for 2 weeks. They were then randomly divided into four groups, and had different dietary treatments for 8 weeks: one group (Control) continued consuming the chow diet, and the other three groups were fed a HFD (F3282; Bio-Serv) with or without additional supplementation. Among those three groups on the HFD, one group was fed HFD only (HFD control), another group was fed HFD with the addition of RES (150 mg/kg; Sigma-Aldrich, St. Louis, MO) for the last 15 days, and the third group was fed HFD with the addition of nicotinamide (NAM) (500 mg/kg; Sigma-Aldrich) for the last 15 days. Mice were injected with either PBS or 10 U/kg insulin (Sigma-Aldrich) for 30 min after an 8 h fast in the RES and NAM groups. Subcutaneous adipose fat, plasma, or serum was immediately removed for p-Akt2 and glucose measurements. For other measurements, adipose tissue, plasma, or serum was collected after insulin treatment for 24 h (24). The ambient temperature of the animal room was maintained at 25 ± 1°C and humidity at 55 ± 5% with a 12 h light/dark cycle. On the last day, mice were euthanized by an overdose of ethyl ether. For in vitro study, differentiated preadipocytes were pretreated with RES and NAM for 48 h, and after 3 h of serum-starvation were treated with 10 nM insulin for 30 min. Rapamycin used in the measurements was purchased from Sigma-Aldrich.

Metabolic phenotyping

Body weight and food intake were recorded once a week, and the Lee index was calculated using the following equation (25):

$$\text{Lee index} = \frac{\sqrt[3]{\text{Body weight (g)}}}{\text{Naso-anal length (cm)}} \times 1{,}000$$

Perinephric fat, epididymis fat, and subcutaneous fat were harvested and weighed on the last day of treatment. Plasma TG and glucose concentrations were measured using a TG determination kit and glucose (HK) assay kit (Sigma-Aldrich), respectively. The plasma concentrations of inducible nitric oxide synthase (iNOS), leptin, and interleukin-6 (IL-6) were detected using commercial ELISA kits from R&D and Cell Signaling Technology (Boston, MA) and Abcam (Cambridge, UK), respectively.

Primary preadipocyte culture and differentiation

Primary preadipocytes from subcutaneous white adipose tissue were isolated and cultured according to the method described previously (26). Preadipocytes were plated onto 35 mm primary culture dishes. The differentiation of preadipocytes was then performed as follows: Cells grown to 100% confluence (day 0) were exposed to induction DMEM/F12 containing dexamethasone (1 μM; Sigma-Aldrich), insulin (10 μg/ml; Sigma-Aldrich), IBMX (0.5 mM; Sigma-Aldrich), and 10% FBS. Four days after the induction (from day 2), cells were maintained in the induction medium containing insulin (10 μg/ml; Sigma-Aldrich) and 10% FBS until the day of harvest.

Materials and vectors

Differentiated preadipocytes were treated with 100 μM RES or 500 μM NAM for 48 h. Plasmid vectors of His-Sirt1 (overexpression vector of Sirt1 with tag-His), Sirt1 (overexpression vector of Sirt1), His-Akt2 (overexpression vector of Akt2 with tag-His), and Akt2 (overexpression vector of Akt2) were all constructed in our laboratory. Lentiviral shRNA vector for Sirt1 (sh-Sirt1) was purchased from Gene Pharma (Shanghai, China). The lentiviral vector expressing a mutant Akt2 construct (Akt2-mutant) was generated by introducing seven silent point mutations in the Akt2 cDNA coding sequence by Gene Pharma. Plasmid vectors were transfected with X-tremeGENE™ transfection reagent (Roche, Basel, Switzerland) at a ratio of 3:1 (X-tremeGENE™ reagent: DNA) for 24–48 h before measurements of mRNA and protein. In addition, differentiated preadipocytes were infected with lentiviral vectors of Sirt1 and mutant-Akt2 for 48 h at the titer of 1×10^9 IFU/ml for further detection.

Cell viability and Oil Red O staining

Cell viability was measured by Cell Counting Kit 8 (CCK-8; Vazyme, Nanjing, China) as described in our previous publication (27). In brief, cells were seeded in a 96-well plate at a density of 5×10^3 and cultured for 12 h. Then 10 μl kit buffer was added into each well and incubated at 37°C for 1 h. Absorbance was quantified at 450 nm by Vector 5 (Bio-Tek, Winooski, VT). Lipid droplets were stained with Oil Red O staining as described in our previous publication (28). In brief, the fixed cells were washed three times with PBS and stained with a working solution of Oil Red O for 30 min at room temperature, and then washed with deionized water and images of the stained cells were viewed under an inverted microscope (Nikon Instruments Europe BV, UK).

Immunoprecipitation using primary antibodies

Differentiated preadipocytes were pretransfected with plasmids using 3 μl X-tremeGENE™ transfection reagent (Roche) per microgram of plasmids. Whole cell lysate was harvested in lysis buffer 48 h post transfection. The supernatant of whole cell lysate was precleaned with protein A (for rabbit primary antibody; Invitrogen, Carlsbad, CA) for 2 h and incubated with 4 μg primary antibody overnight at 4°C with shaking. Immune complexes were pulled down with protein A for 2 h at 4°C with shaking. Beads were washed once with lysis buffer, three times with washing buffer, followed by SDS-PAGE and Western blot analysis.

Real-time PCR analysis

Total RNA was extracted from subcutaneous adipose tissue or differentiated preadipocytes with TRIpure reagent kit (Takara, Dalian, China) and 400 ng of total RNA was reverse transcribed using the M-MLV reverse transcriptase kit (Takara). Primers were synthesized by Shanghai Sangon Ltd. (Shanghai, China). Quantitative PCR was performed in 25 μl reactions containing specific primers and SYBR Premix EX Taq (Takara). The levels of mRNAs were normalized to β-actin. The expression of genes was analyzed by method of $2^{-\Delta\Delta Ct}$.

Protein extraction and Western blot analysis

Differentiated preadipocytes were lysed in RIPA buffer for 40 min at 4°C. The lysate was centrifuged at 12,000 *g* for 15 min at 4°C, and the supernatant was used for protein assay. Proteins (50 μg) in the supernatant were separated by electrophoresis on 12% and 5% SDS-PAGE gels using slab gel apparatus and then transferred to PVDF nitrocellulose membranes (Millipore, Boston, MA) blocked with 5% skim milk powder/Tween 20/TBST at room

temperature for 2 h. Primary antibodies against raptor, p-mTOR^{Ser2448}, mTOR^{Ser2448}, p-S6K1^{Thr389}, S6K1^{Thr389}, and GAPDH were purchased from Bioworld (Nanjing, China). Antibodies against Sirt1, leptin, IL-6, MCP-1, TNF-α, p-Akt2^{Ser473}, Akt2, and target-His were from Abcam. Antibody against iNOS was from Cell Signaling Technology (Danvers, MA), and Akt2-specific inhibitor, CCT128930, was from Abcam and rapamycin was from Sigma-Aldrich. Membranes were first incubated with primary antibodies at 4°C overnight, followed with HRP-conjugated secondary antibodies (Boaoshen, China) for 2 h at room temperature. Proteins were visualized using chemiluminescent peroxidase substrate (Millipore) and quantified using ChemiDoc XRS system (Bio-Rad, Hercules, CA).

Statistical analysis

Statistical analyses were conducted using SAS v8.0 (SAS Institute, Cary, NC). Data were analyzed using one-way ANOVA. Comparisons among individual means were made by Fisher's least significant difference (LSD). Data are presented as mean ± SD. $P < 0.05$ was considered to be significant.

RESULTS

Sirt1 reduced adipose deposition and decreased Akt2 level in obese mice

The body weights of mice are shown in **Fig. 1A**. Mice on HFD for 8 weeks had significantly higher body weight than that of week 6. The Lee index and food intake were higher compared with those of mice on chow diet (Fig. 1A–C). The Sirt1 mRNA level in the adipose tissue was reduced, but Akt2 and IL-6 mRNA levels were increased (Fig. 1D). Addition of RES significantly reduced the body weight, whereas addition of NAM had an opposite effect (Fig. 1E). No difference in food intake was found among RES, NAM, and HFD control

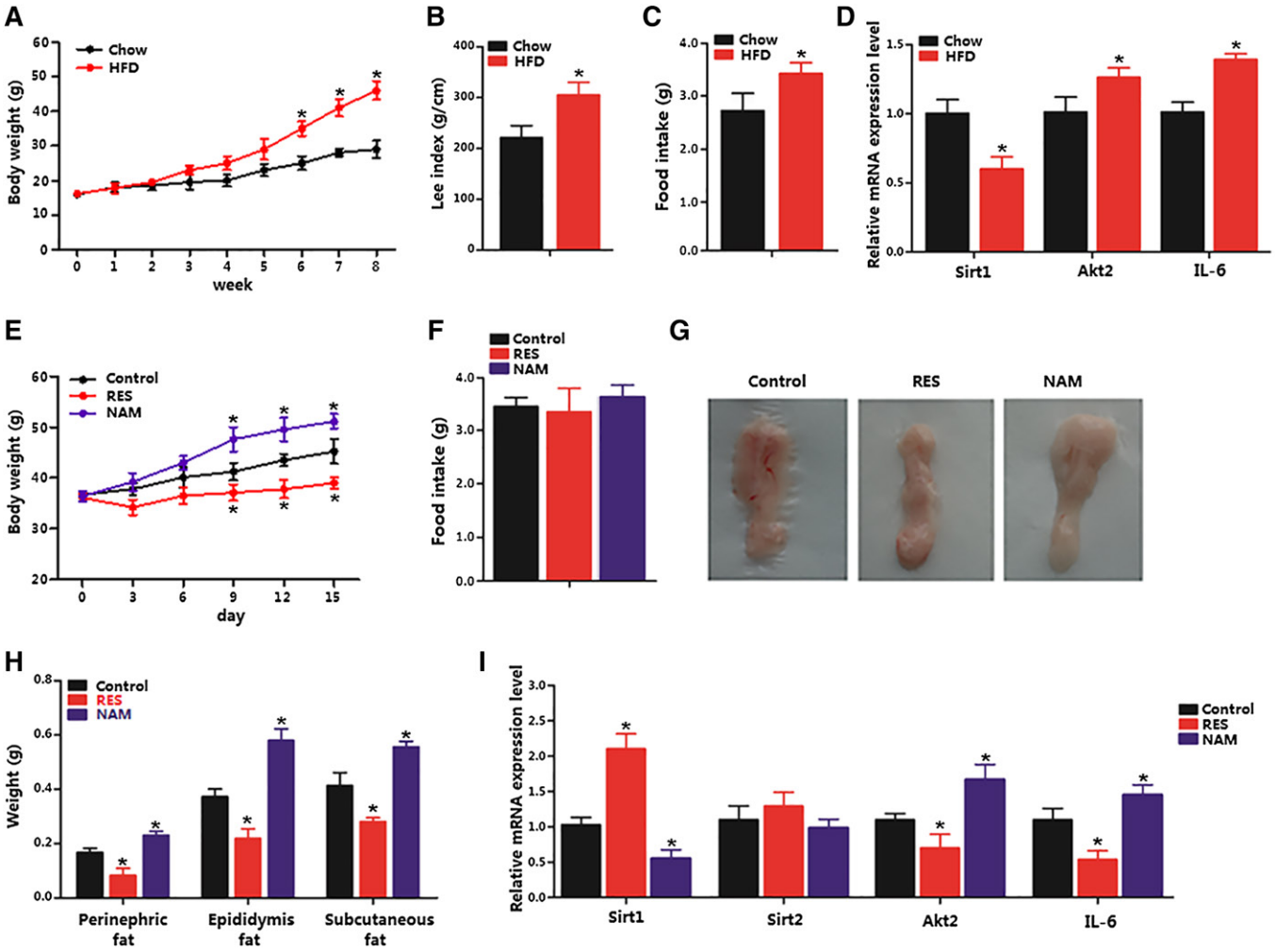

Fig. 1. Sirt1 reduced adipose deposition and decreased Akt2 level in obese mice. Mice were fed either chow diet (n = 20) or HFD for 8 weeks, and mice on HFD diet had daily addition of RES or NAM (n = 20) over the last 15 days and an insulin injection over 30 min after 8 h fasting on the last day. A: Body weight gain of mice on chow diet or HFD (n = 20). B: Lee index of mice on chow diet or HFD. C: Food intake of mice on chow diet or HFD (n = 20). D: Relative mRNA levels of Sirt1, Akt2, and IL-6 in subcutaneous adipose tissue of mice on HFD (n = 20). E: Body weight gain of mice on HFD with addition of RES or NAM over the last 15 days (n = 6). F: Food intake of mice on HFD with addition of RES or NAM over the last 15 days (n = 6). G: Representative images of subcutaneous fat of mice on HFD with addition of RES or NAM over the last 15 days (n = 6). H: Weights of perinephric fat, epididymis fat, and subcutaneous fat of mice on HFD with addition of RES or NAM over the last 15 days (n = 6). I: Relative mRNA level of Sirt1, Sirt2, Akt2, and IL-6 in subcutaneous adipose tissue of mice on HFD with addition of RES or NAM over the last 15 days (n = 6). Values are mean ± SD. *$P < 0.05$ as compared with the corresponding control.

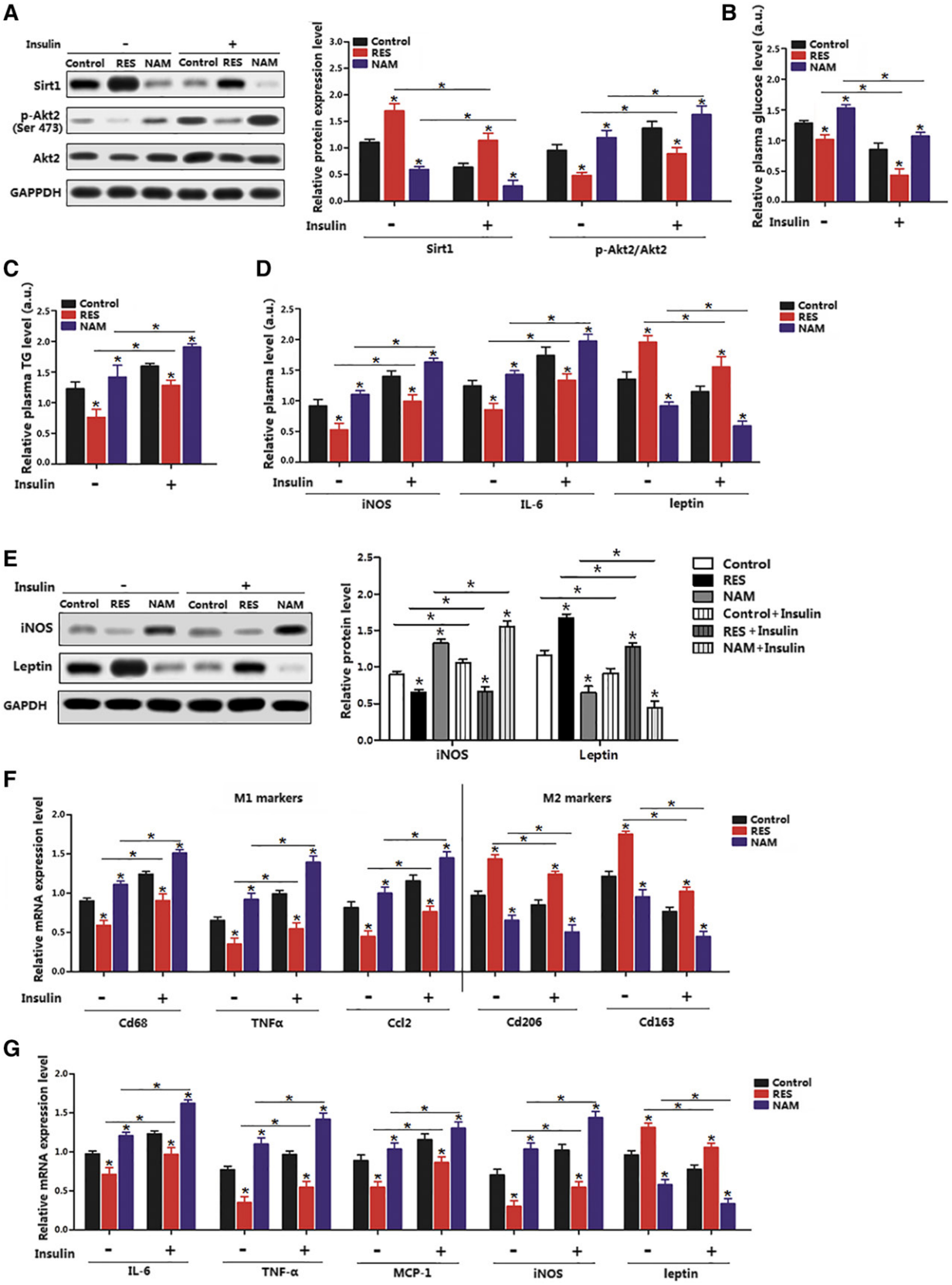

Fig. 2. Sirt1 inhibited adipose inflammation and insulin-stimulated Akt2 activation. A: Immunoblots of Sirt1 and p-Akt2^{Ser473} of subcutaneous adipose tissue in mice on HFD with addition of RES or NAM over the last 15 days; insulin was injected for 30 min (n = 6). B: Relative plasma glucose concentration of mice on HFD with addition of RES or NAM over the last 15 days; insulin was injected for 30 min (n = 6). The actual glucose content in the control group, RES group, and NAM group without insulin was 9.11 mmol/l, 7.84 mmol/l, and 10.63 mmol/l; the actual glucose content in the control group, RES group, and NAM group with insulin treatment was 5.47 mmol/l, 4.64 mmol/l, and 8.72 mmol/l. C: Relative plasma TG concentration 24 h after the insulin injection in mice on HFD with addition of RES or NAM over

groups (Fig. 1F). Fat pads from three locations (epididymal, perinephric, subcutaneous) all weighed less in RES-fed mice (Fig. 1G, H). Moreover, RES increased Sirt1 expression but decreased Akt2 and IL-6 expression (Fig. 1I). Thus, the data elucidate that RES reduced body weight of mice and inhibited inflammation by elevating Sirt1 and reducing Akt2.

Sirt1 inhibited adipose inflammation and insulin-stimulated Akt2 activation

We next addressed whether the alternation of Sirt1 impaired Akt2, and whether Sirt1 functioned in obesity-related inflammation. The RES treatment increased the Sirt1 level and decreased Akt2 activity in the insulin-stimulated adipose tissue, whereas NAM had the opposite effects (**Fig. 2A**). Plasma TG and glucose levels were both reduced in RES mice (Fig. 2B, C). In addition, RES also decreased plasma iNOS and IL-6 levels, which were elevated after the insulin stimulation (Fig. 2D). The protein level of iNOS was decreased by RES, but leptin was increased (Fig. 2E). Consistently, RES reduced macrophage type I markers, but elevated macrophage type II markers, even when treated by insulin (Fig. 2F). The mRNA levels of inflammation marker genes, such as IL-6, TNF-α, MCP-1, and iNOS, were decreased, but increased by the insulin stimulation (Fig. 2G). All these results suggest that Sirt1 and Akt2 functioned inversely in the regulation of adipose inflammation.

Sirt1 physically interacted with Akt2 in reducing mouse adipocyte inflammation

The interaction between Sirt1 and Akt2 on inflammation was examined at protein level. The transfection efficiency of plasmid vectors in differentiated preadipocytes is shown in supplemental Fig. S1. Basal Akt2 protein interacted with transfected Sirt1 protein in differentiated preadipocytes (**Fig. 3A**). The RES enhanced this interaction significantly, but NAM blocked the interaction between Sirt1 and Akt2 (Fig. 3A, C). The insulin treatment enhanced the interaction between Sirt1 and Akt2, as shown in Fig. 3B. The Akt2 phosphorylation level was decreased in a time-dependent manner by RES treatment, while NAM treatment showed the opposite result (Fig. 3D, E), confirming that Sirt1 down-regulated Akt2 activity. The Akt2-specific inhibitor, CCT128930, significantly decreased the Akt2 phosphorylation level and reduced the levels of IL-6, MCP-1, TNF-α, and iNOS (Fig. 3F, G). Consistently, CCT128930 treatment had an additive effect on the reduced adipose inflammation by Sirt1 (Fig. 3H). However, in differentiated preadipocytes transfected with Akt2 dead mutant vector and Sirt1 vector, adipocyte inflammation was restored (Fig. 3I). These results together reveal that RES decreases adipose inflammation by promoting the interaction between Sirt1 and Akt2.

Sirt1 reduced adipocyte inflammation by inhibiting the Akt2/mTOR pathway

Differentiated preadipocytes were induced in this experiment. RES inhibited adipose accumulation and NAM promoted adipose accumulation; PPARγ and FAS levels were decreased with RES addition; in contrast, NAM increased their levels (**Fig. 4A, B**). RES reduced the expression of IL-6, TNF-α, and MCP-1, while it enhanced the expression of leptin with or without the insulin treatment (Fig. 4C). To further illustrate the role of Sirt1 in RES-reduced inflammation, the interference or overexpression vectors of Sirt1 were used. Figure 4D demonstrates that overexpression of Sirt1 almost completely inhibited IL-6 and MCP-1 with the addition of RES, while sh-Sirt1 recovered the levels of IL-6 and MCP-1 (Fig. 4D). The reduction of raptor and p-mTOR activity indicated that Sirt1 functioned via the mTOR signal pathway (Fig. 4E). Despite insulin stimulation enhancing Akt2 activity, Sirt1 decreased Akt2 activity and reduced the expression levels of raptor and p-mTOR (Fig. 4E). Thus, these results indicate that RES inhibited adipose inflammation by activating the Sirt1/Akt2/mTOR pathway.

The mTOR/S6K1 pathway was essential for regulation of Sirt1 in adipocyte inflammation

The essentiality of mTORC1 signal for Sirt1-regulated inflammation was determined by measuring the phosphorylation levels of $mTOR^{Ser2448}$ and $S6K1^{Thr389}$ with or without RES/NMA. Interestingly, RES reduced the activity of $p\text{-}mTOR^{Ser2448}$ and $p\text{-}S6K1^{Thr389}$, whereas NAM increased those activities (**Fig. 5A**). A further addition of rapamycin, the mTORC1-specific inhibitor, accentuated the reduction of mTOR activity, while the addition of insulin restored the levels of $p\text{-}mTOR^{Ser2448}$ and $p\text{-}S6K1^{Thr389}$ (Fig. 5A). Additionally, the RES resulted in inactivation of the mTOR signal pathway and strongly reduced the expression of IL-6, iNOS, and MCP-1; further addition of insulin elevated expression of these genes (Fig. 5B). Thus, the

the last 15 days (n = 6). The absolute TG content in the control group without insulin was 1 mmol/l, in the RES group without insulin was 0.75 mmol/l, in the NAM group without insulin was 1.3 mmol/l. The absolute TG content in the control group with insulin treatment was 1.5 mmol/l, in the RES group with insulin treatment was 1.1 mmol/l, in NAM group with insulin treatment was 1.7 mmol/l. D: Relative plasma iNOS, IL-6, and leptin concentration 24 h after insulin injection in mice on HFD with addition of RES or NAM over the last 15 days (n = 6). Absolute plasma iNOS content in the control group, RES group, and NAM group without insulin was 6.2 U/ml, 4.11 U/ml, and 8.42 U/ml; and in the control group, RES group, and NAM group with insulin treatment was 9.31 U/ml, 6.25 U/ml, and 10.3 U/ml. Absolute plasma IL-6 content in the control group, RES group, and NAM group without insulin was 16.2 pg/ml, 13.31 pg/ml, and 19 pg/ml; and in the control group, RES group, and NAM group with insulin treatment was 21.3 pg/ml, 15.7 pg/ml, and 24.8 pg/ml. Absolute plasma leptin content in the control group, RES group, and NAM group without insulin was 7.3 ng/ml, 11 ng/ml, and 5.2 ng/ml; and in the control group, RES group, and NAM group with insulin treatment was 6.11 ng/ml, 8.5 ng/ml, and 4.2 ng/ml. E: Immunoblots of iNOS and leptin 24 h after the insulin injection in mice on HFD with addition of RES or NAM over the last 15 days (n = 6). F: mRNA levels of macrophage type I (M1) or macrophage type II (M2) macrophage markers 24 h after the insulin injection in mice on HFD with addition of RES or NAM over the last 15 days (n = 6). G: mRNA levels of inflammation markers 24 h after the insulin injection in mice on HFD with addition of RES or NAM over the last 15 days (n = 6). Control: fed HFD only. Values are mean ± SD. $*P < 0.05$ as compared with the corresponding control.

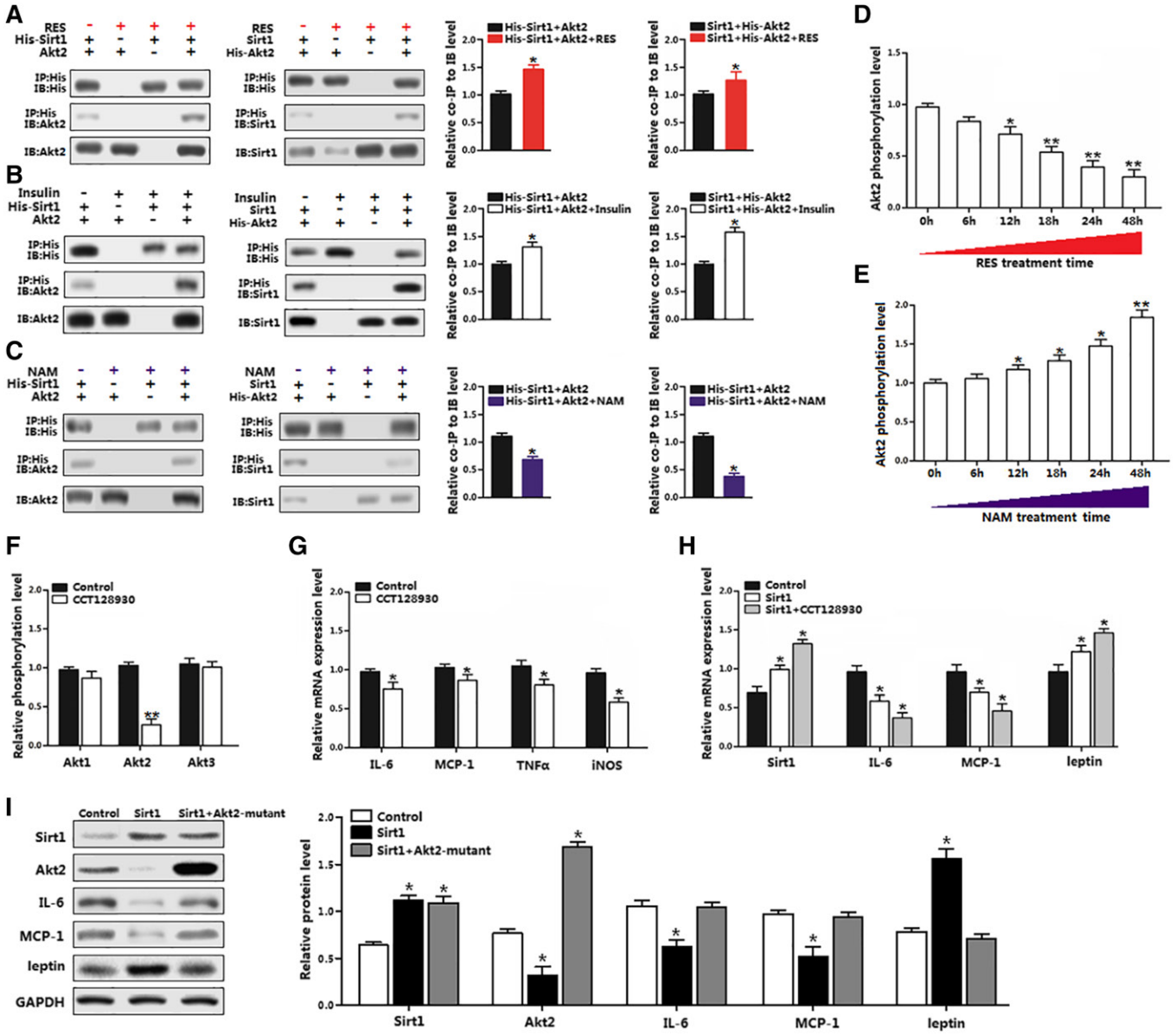

Fig. 3. Sirt1 interacted with Akt2 in reducing mouse adipocyte inflammation. A: Interaction between Sirt1 and Akt2 was strengthened by RES; quantitative analysis ratio of co-immunoprecipitation (coIP) level to immunoblot (IB) level from lane 1 and lane 4 in each panel (n = 3). B: Interaction between Sirt1 and Akt2 was strengthened by insulin; quantitative analysis ratio of coIP level to IB level from lane 1 and lane 4 in each panel (n = 3). C: Interaction between Sirt1 Akt2 was blocked by NAM; quantitative analysis ratio of coIP level to IB level from lane 1 and lane 4 in each panel (n = 3). D: Phosphorylation levels of Akt2 in differentiated preadipocytes from 0 h up to 48 h with RES treatment (n = 3). E: Phosphorylation levels of Akt2 in differentiated preadipocytes from 0 h up to 48 h with NAM treatment (n = 3). F: Relative phosphorylation levels of Akt1, Akt2, and Akt3 with 5 μM CCT128930 treatment for 30 min in differentiated preadipocytes (n = 3). G: mRNA levels of inflammation markers in differentiated preadipocytes treated with 5 μM CCT128930 for 30 min (n = 3). H: mRNA levels of Sirt1, IL-6, MCP-1, and leptin in differentiated preadipocytes pretransfected with Sirt1 and incubated with 5 μM CCT128930 for 30 min (n = 3). I: Immunoblots of Sirt1, Akt2, IL-6, MCP-1, and leptin in differentiated preadipocytes infected with Sirt1 and Akt2-mutant (n = 3). Sirt1, overexpression vector of Sirt1; His-Sirt1, overexpression vector of Sirt1 with tag-His; Akt2, overexpression vector of Akt2; His-Akt2, overexpression vector of Akt2 with tag-His; Akt2-mutant, lentiviral vector expressing mutant Akt2. The treating concentrations of RES and NAM were 100 μM and 500 μM, respectively, in differentiated preadipocytes. Values are mean ± SD. *$P < 0.05$ and **$P < 0.01$ as compared with the control.

mTORC1/S6K1 signal pathway was essential for adipocyte inflammation.

DISCUSSION

Chronic low-grade tissue inflammation is an important etiologic component of obesity-related diseases like insulin resistance, metabolic syndrome, and type 2 diabetes (7, 29, 30). RES is a natural plant polyphenol that prevents obesity-related chronic diseases through reducing the synthesis of lipids (31). Activation of Sirt1 by RES can lead to an enhancement of glucose tolerance and insulin sensitivity (10, 32). In the current study, we found that HFD reduced the expression of Sirt1 and elevated Akt2 expression. The reversal relationship between Sirt1 and Akt2 expressions was also found by RES treatment. This reversal relationship

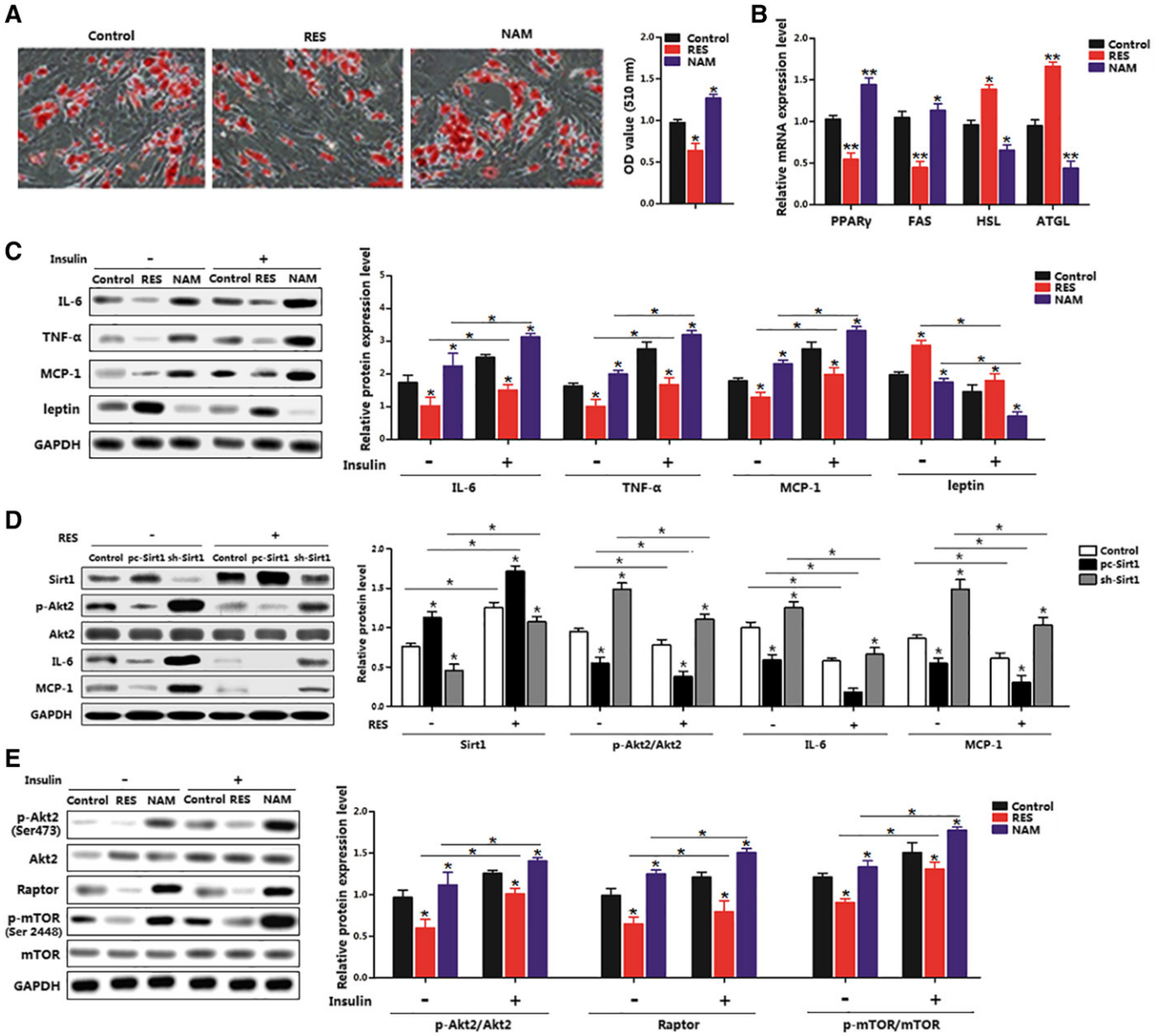

Fig. 4. Sirt1 reduced adipocyte inflammation by inhibiting the Akt2/mTOR pathway. A: Oil Red O staining of differentiated preadipocytes for 8 days with RES or NAM treatment for 48 h (n = 3). B: Expression of adipogenic genes in differentiated preadipocytes with RES or NAM treatment for 48 h (n = 3). C: Immunoblots of inflammation markers in differentiated preadipocytes treated with RES or NAM for 48 h, followed with 10 nM insulin for 30 min (n = 3). C: Immunoblots of mTORC1 signaling differentiated preadipocytes treated with RES or NAM for 48 h, followed with 10 nM insulin for 30 min (n = 3). D: Immunoblots of Sirt1, p-Akt2, IL-6, and MCP-1 in differentiated preadipocytes pretreated with pc-Sirt1 or sh-Sirt1, and then with RES for 48 h (n = 3). E: Immunoblots of p-Akt2 and mTORC1 signaling in differentiated preadipocytes pretreated with RES or NAM for 48 h, and then with 10 nM insulin for 30 min (n = 3). pc-Sirt1: same vector as Sirt1, overexpression vector of Sirt1. sh-Sirt1: lentiviral vector containing shRNA constructs against Sirt1. The treating concentrations of RES and NAM were 100 μM and 500 μM, respectively, in differentiated preadipocytes. Values are mean ± SD. *$P < 0.05$ and **$P < 0.01$ as compared with the control.

could be altered by RES and NAM. These results are consistent with previous reports (33, 34). Thus, Sirt1 is an important target to combat metabolic disorders, and for potential therapeutic interventions.

Insulin is a key regulator of glucose homeostasis, and its absence is lethal in human cells (35). The downstream effectors of insulin signal, Akts, are activated and affect metabolism, proliferation, apoptosis, growth, and inflammation of cells (36). Inhibiting the Akt signal pathway increases anti-inflammatory effects and decelerates the metabolic syndrome. The Sirt1 level is increased in response to calorie restriction, the most consistent intervention to increase lifespan and protect against deteriorations in biological functions of many key metabolic tissues (37, 38). Using immunoprecipitation, we found that Sirt1 directly bound to Akt2. Our finding is consistent with the result found in porcine adipogenesis (22). Interestingly, RES promoted the interaction between Sirt1 and Akt2, but NAM reduced this interaction in this study. Phosphoinositide 3-kinase (PI3K), Akt, and their downstream kinase, mTOR, are implicated in insulin resistance, metabolic dysfunction, and inflammation (15). Thus, we focused on the influence

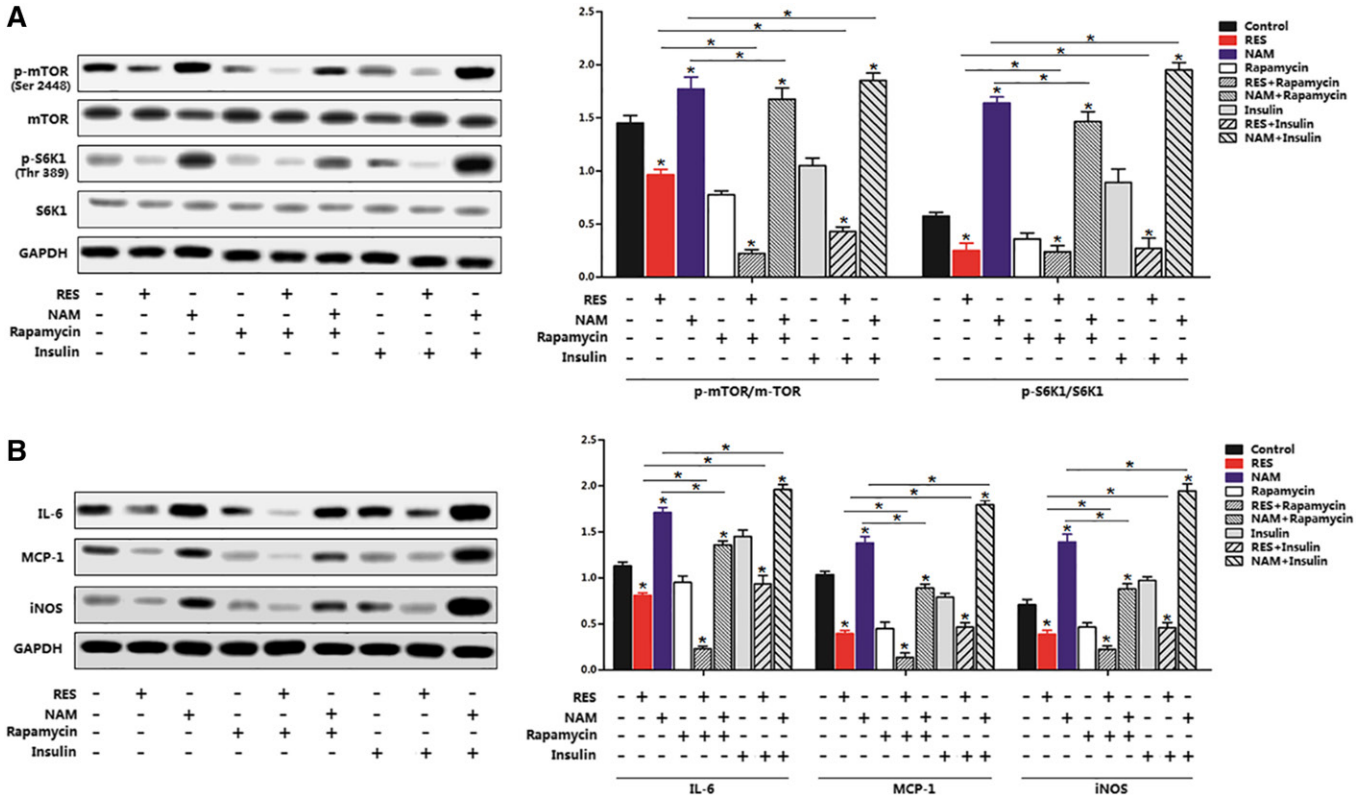

Fig. 5. The mTOR/S6K1 pathway was essential for regulation of Sirt1 in adipocyte inflammation. A: Phosphorylation and protein levels of mTOR and S6K1 in differentiated preadipocytes pretreated with RES or NAM for 48 h, and then with 5 nM rapamycin for 60 min, followed with 10 nM insulin for 30 min (n = 3). B: Immunoblots of inflammation markers in differentiated preadipocytes pretreated with RES or NAM for 48 h, and then with 5 nM rapamycin for 60 min, followed with 10 nM insulin for 30 min (n = 3). The treating concentrations of RES and NAM were 100 μM and 500 μM, respectively, in differentiated preadipocytes. Values are mean ± SD. $*P < 0.05$ as being compared with the control.

of Sirt1 and Akt2 interaction on the mTOR pathway, and found that Sirt1 inhibited raptor expression and the phosphorylation of mTOR. The result implies that the mTORC1 pathway is involved in the regulation of adipose inflammation by Sirt1 and Akt2 interaction.

mTOR is a serine/threonine protein kinase that regulates protein synthesis (39). Studies report that activation of the mTOR pathway plays a key role in TNF-α-induced inflammatory cascades (40) and is also implicated in inflammation-related diseases. mTORC1 is highly activated in tissues of obese humans and HFD-fed rodents (19, 41). Inhibition of mTORC1 promotes triacylglycerol lipolysis that releases free fatty acids, blocks adipogenesis, and impairs the maintenance of fat cells (42, 43). Recent studies have demonstrated that the most common cancer-promoting signaling event that converges on mTORC1 is aberrant activation of Akt kinase (44). Our data showed that Sirt1 decreased the phosphorylation level of mTOR/S6K1, and this effect was attenuated by rapamycin, which specifically inhibited mTOR signal. Conversely, the insulin treatment elevated this effect. All of these results indicate that the mTOR/S6K1 pathway is involved in the regulation of adipose inflammation by the interaction between Sirt1 and Akt2.

CONCLUSIONS

In conclusion, the findings of this study demonstrate that: RES inhibits adipose inflammation by activating Sirt1 and promoting the interaction between Sirt1 and Akt2; the mTOR/S6K1 pathway is involved in this interaction; and inhibition of this pathway alleviated adipose inflammation (**Fig. 6**). These findings shed a new light that intracellular pathways could be a target for developing prevention or treatment of obesity-associated endocrine and metabolic diseases.

The authors express their gratitude to Professor C. Y. Hu, Dr. Douglas L. Vincent, and Assistant Professor Rajesh Jha from the University of Hawaii at Manoa and Shimin Liu from for University of Western Australia for helping in the revision of the manuscript.

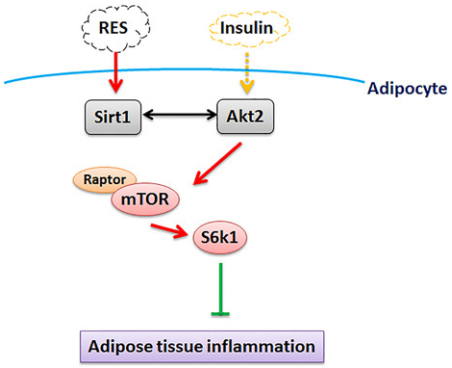

Fig. 6. Sirt1 interacts with Akt2 in the regulation of adipocyte inflammation via inhibiting the mTORC1/S6K1 signal pathway; Akt2 plays an important role in the regulation of RES on Sirt1.

REFERENCES

1. Rodgers, J. T., C. Lerin, W. Haas, S. P. Gygi, B. M. Spiegelman, and P. Puigserver. 2005. Nutrient control of glucose homeostasis through a complex of PGC-1α and SIRT1. *Nature.* **434:** 113–118.
2. Picard, F., M. Kurtev, N. Chung, A. Topark-Ngarm, T. Senawong, and R. M. De Oliveira. 2004. Sirt1 promotes fat mobilization in white adipocytes by repressing PPAR-γ. *Nature.* **429:** 771–776.
3. Yoshizaki T., J. C. Milne, T. Imamura, S. Schenk, N. Sonoda, J. L. Babendure, J. C. Lu, J. J. Smith, M. R. Jirousek, and J. M. Olefsky. 2009. SIRT1 exerts anti-inflammatory effects and improves insulin sensitivity in adipocytes. *Mol. Cell. Biol.* **29:** 1363–1374.
4. Hotamisligil, G. S., P. Arner, J. F. Caro, R. L. Atkinson, and B. M. Spiegelman. 1995. Increased adipose tissue expression of tumor necrosis factor-alpha in human obesity and insulin resistance. *J. Clin. Invest.* **95:** 2409–2415.
5. Gillum, M. P., M. E. Kotas, D. M. Erio, R. P. Kursawe, and K. T. Chatterjee. 2011. Sirt1 regulates adipose tissue inflammation. *Diabetes.* **60:** 3235–3245.
6. Guarente, L. 2006. Sirtuins as potential targets for metabolic syndrome. *Nature.* **444:** 868–874.
7. Yoshizaki, T., S. Schenk, T. Imamura, J. L. Babendure, N. Sonoda, and E. J. Bae. 2010. SIRT1 inhibits inflammatory pathways in macrophages and modulates insulin sensitivity. *Am. J. Physiol. Endocrinol. Metab.* **298:** E419–E428.
8. Purushotham, A., T. T. Schug, Q. Xu, S. Surapureddi, X. Guo, and X. Li. 2009. Hepatocyte-specific deletion of SIRT1 alters fatty acid metabolism and results in hepatic steatosis and inflammation. *Cell Metab.* **9:** 327–338.
9. Park, S. J., F. Ahmad, A. Philp, K. Baar, T. Williams, H. Luo, H. Ke, H. Rehmann, R. Taussig, and A. L. Brown. 2012. Resveratrol ameliorates aging-related metabolic phenotypes by inhibiting cAMP phosphodiesterases. *Cell.* **148:** 421–433.
10. Lagouge, M., C. Argmann, Z. Gerhart-Hines, H. Meziane, C. Lerin, F. Daussin, N. Messadeq, J. Milne, P. Lambert, and P. Elliott. 2006. Resveratrol improves mitochondrial function and protects against metabolic disease by activating SIRT1 and PGC-1α. *Cell.* **127:** 1109–1122.
11. Chen, M. L., L. Yi, X. Jin, X. Y. Liang, Y. Zhou, T. Zhang, Q. Xie, X. Zhou, H. Chang, and Y. J. Fu. 2013. Resveratrol attenuates vascular endothelial inflammation by inducing autophagy through the cAMP signaling pathway. *Autophagy.* **9:** 2033–2045.
12. Nwachukwu, J. C., S. Srinivasan, N. E. Bruno, A. A. Parent, T. S. Hughes, J. A. Pollock, O. Gjyshi, V. Cavett, J. Nowak, and R. D. Garcia-Ordonez. 2014. Resveratrol modulates the inflammatory response via an estrogen receptor-signal integration network. *eLife.* **3:** e02057.
13. Fischer-Posovszky, P., V. Kukulus, D. Tews, T. Unterkircher, K. M. Debatin, S. Fulda, and M. Wabitsch. 2010. Resveratrol regulates human adipocyte number and function in a Sirt1-dependent manner. *Am. J. Clin. Nutr.* **92:** 5–15.
14. Bodine, S. C., T. N. Stitt, M. Gonzalez, W. O. Kline, G. L. Stover, and R. Bauerlein. 2001. Akt/mTOR pathway is a crucial regulator of skeletal muscle hypertrophy and can prevent muscle atrophy in vivo. *Nat. Cell Biol.* **3:** 1014–1019.
15. Liu, M., J. Bai, S. He, R. Villarreal, D. Hu, and C. Zhang. 2014. Grb10 promotes lipolysis and thermogenesis by phosphorylation-dependent feedback inhibition of mTORC1. *Cell Metab.* **19:** 967–980.
16. Guertin, D. A., and D. M. Sabatini. 2007. Defining the role of mTOR in cancer. *Cancer Cell.* **12:** 9–22.
17. Sarbassov, D. D., D. A. Guertin, S. M. Ali, and D. M. Sabatini. 2005. Phosphorylation and regulation of Akt/PKB by the rictor-mTOR complex. *Science.* **307:** 1098–1101.
18. Ravikumar, B., C. Vacher, Z. Berger, J. E. Davies, S. Luo, and L. G. Oroz. 2004. Inhibition of mTOR induces autophagy and reduces toxicity of polyglutamine expansions in fly and mouse models of Huntington disease. *Nat. Genet.* **36:** 585–595.
19. Tilg, H., and A. R. Moschen. 2006. Adipocytokines: mediators linking adipose tissue, inflammation and immunity. *Nat. Rev. Immunol.* **6:** 772–783.
20. Han, M. S., D. Y. Jung, C. Morel, S. A. Lakhani, J. K. Kim, R. A. Flavell, and R. J. Davis. 2013. JNK expression by macrophages promotes obesity-induced insulin resistance and inflammation. *Science.* **339:** 218–222.
21. Jiang, H., M. Westerterp, C. Wang, Y. Zhu, and D. Ai. 2014. Macrophage mTORC1 disruption reduces inflammation and insulin resistance in obese mice. *Diabetologia.* **57:** 2393–2404.
22. Pang, W., Y. Wang, N. Wei, R. Xu, Y. Xiong, and P. Wang. 2013. Sirt1 inhibits akt2-mediated porcine adipogenesis potentially by direct protein-protein interaction. *PLoS One.* **8:** e71576.
23. Busch, F., A. Mobasheri, P. Shayan, R. Stahlmann, and M. Shakibaei. 2012. Sirt-1 is required for the inhibition of apoptosis and inflammatory responses in human tenocytes. *J. Biol. Chem.* **287:** 25770–25781.
24. Chen, M., J. Breslow, W. Li, and T. Leff. 1994. Transcriptional regulation of the apoC-III gene by insulin in diabetic mice: correlation with changes in plasma triglyceride levels. *J. Lipid Res.* **35:** 1918–1924.
25. Lee, M. O. 1929. Determination of the surface area of the white rat with its application to the expression of metabolic results. *Am. J. Physiol.* **89:** 24–33.
26. Gan, L., Z. Liu, W. Cao, Z. Zhang, and C. Sun. 2015. FABP4 reversed the regulation of leptin on mitochondrial fatty acid oxidation in mice adipocytes. *Sci. Rep.* **5:** 13588.
27. Gan, L., Z. Liu, W. Jin, Z. Zhou, and C. Sun. 2015. Foxc2 enhances proliferation and inhibits apoptosis through activating Akt/mTORC1 signaling pathway in mouse preadipocytes. *J. Lipid Res.* **56:** 1471–1480.
28. Gan, L., J. Yan, Z. Liu, M. Feng, and C. Sun. 2015. Adiponectin prevents reduction of lipid-induced mitochondrial biogenesis via AMPK/ACC2 pathway in chicken adipocyte. *J. Cell. Biochem.* **116:** 1090–1100.
29. Arkan, M. C., A. L. Hevener, F. R. Greten, S. Maeda, Z. W. Li, and J. M. Long. 2005. IKK-β links inflammation to obesity-induced insulin resistance. *Nat. Med.* **11:** 191–198.
30. Hotamisligil, G. S. 2006. Inflammation and metabolic disorders. *Nature.* **444:** 860–867.
31. Baur, J. A., K. J. Pearson, N. L. Price, H. A. Jamieson, C. Lerin, and A. Kalra. 2006. Resveratrol improves health and survival of mice on a high-calorie diet. *Nature.* **444:** 337–342.
32. Milne, J. C., P. D. Lambert, S. Schenk, D. P. Carney, J. J. Smith, and D. J. Gagne. 2007. Small molecule activators of SIRT1 as therapeutics for the treatment of type 2 diabetes. *Nature.* **450:** 712–716.
33. Timmers, S., E. Konings, L. Bilet, R. H. Houtkooper, T. van de Weijer, G. H. Goossens, J. Hoeks, S. van der Krieken, D. Ryu, and S. Kersten. 2011. Calorie restriction-like effects of 30 days of resveratrol supplementation on energy metabolism and metabolic profile in obese humans. *Cell Metab.* **14:** 612–622.
34. Feige, J. N., M. Lagouge, C. Canto, A. Strehle, S. M. Houten, J. C. Milne, P. D. Lambert, C. Mataki, P. J. Elliott, and J. Auwerx. 2008. Specific SIRT1 activation mimics low energy levels and protects against diet-induced metabolic disorders by enhancing fat oxidation. *Cell Metab.* **8:** 347–358.
35. Kadowaki, T., K. Ueki, T. Yamauchi, and N. Kubota. 2012. SnapShot: insulin signaling pathways. *Cell.* **148:** 624.
36. Kidd, L. B., G. A. Schabbauer, J. P. Luyendyk, T. D. Holscher, R. E. Tilley, and M. Tencati. 2008. Insulin activation of the phosphatidylinositol 3-kinase/protein kinase B (Akt) pathway reduces lipopolysaccharide-induced inflammation in mice. *J. Pharmacol. Exp. Ther.* **326:** 348–353.
37. Cohen, H. Y., C. Miller, K. J. Bitterman, N. R. Wall, B. Hekking, and B. Kessler. 2004. Calorie restriction promotes mammalian cell survival by inducing the SIRT1 deacetylase. *Science.* **305:** 390–392.
38. Nisoli, E., C. Tonello, A. Cardile, V. Cozzi, R. Bracale, and L. Tedesco. 2005. Calorie restriction promotes mitochondrial biogenesis by inducing the expression of eNOS. *Science.* **310:** 314–317.
39. Lee, D. F., H. P. Kuo, C. T. Chen, J. M. Hsu, C. K. Chou, and Y. Wei. 2007. IKKβ suppression of TSC1 links inflammation and tumor angiogenesis via the mTOR pathway. *Cell.* **130:** 440–455.
40. Greten, F. R., L. Eckmann, T. F. Greten, J. M. Park, Z. W. Li, and L. J. Egan. 2004. IKKβ links inflammation and tumorigenesis in a mouse model of colitis-associated cancer. *Cell.* **118:** 285–296.
41. Tremblay, F., A. Gagnon, A. Veilleux, A. Sorisky, and A. Marette. 2005. Activation of the mammalian target of rapamycin pathway acutely inhibits insulin signaling to Akt and glucose transport in 3T3–L1 and human adipocytes. *Endocrinology.* **146:** 1328–1337.
42. Chakrabarti, P., T. English, J. Shi, C. M. Smas, and K. V. Kandror. 2010. Mammalian target of rapamycin complex 1 suppresses lipolysis, stimulates lipogenesis, and promotes fat storage. *Diabetes.* **59:** 775–781.
43. Soliman, G. A. 2011. The integral role of mTOR in lipid metabolism. *Cell Cycle.* **10:** 861–862.
44. Shaw, R. J., and L. C. Cantley. 2006. Ras, PI3K and mTOR signaling controls tumour cell growth. *Nature.* **441:** 424–430.